

Cite this: *Chem. Sci.*, 2021, 12, 2242

All publication charges for this article have been paid for by the Royal Society of Chemistry

Received 10th October 2020  
Accepted 19th December 2020

DOI: 10.1039/d0sc05625a

rsc.li/chemical-science

# Accelerated reactions of amines with carbon dioxide driven by superacid at the microdroplet interface†

Kai-Hung Huang, Zhenwei Wei and R. Graham Cooks \*

Microdroplets display distinctive interfacial chemistry, manifested as accelerated reactions relative to those observed for the same reagents in bulk. Carbon dioxide undergoes C–N bond formation reactions with amines at the interface of droplets to form carbamic acids. Electrospray ionization mass spectrometry displays the reaction products in the form of the protonated and deprotonated carbamic acid. Electrosonic spray ionization (ESSI) utilizing carbon dioxide as nebulization gas, confines reaction to the gas–liquid interface where it proceeds much faster than in the bulk. Intriguingly, trace amounts of water accelerate the reaction, presumably by formation of superacid or superbase at the water interface. The suggested mechanism of protonation of CO<sub>2</sub> followed by nucleophilic attack by the amine is analogous to that previously advanced for imidazole formation from carboxylic acids and diamines.

## Introduction

Carbon dioxide is intriguing for its important role in earth science, plant biology, and past and future climates.<sup>1–3</sup> The crucial role of photosynthesis in biology means that carbon dioxide is the key building block for numerous biomolecules. Moreover, the conversion of carbon dioxide into valuable chemicals has been a driving force in fields like organometallic catalysis.<sup>4,5</sup> Environmental damage due to the increasing atmospheric concentrations of carbon dioxide has prompted the development of carbon dioxide capture and storage strategies using absorbents<sup>6–8</sup> which include monoethanolamine,<sup>9</sup> ionic liquids,<sup>10</sup> and metal–organic frameworks.<sup>11,12</sup> As a result of all these considerations, investigations of carbon dioxide chemistry have acquired special significance.<sup>4,13</sup> Amine–carbon dioxide chemistry is a focus of CO<sub>2</sub> capture in industry.

In the past decade, microdroplet reactions have gained attention due to reaction acceleration (increased rate constants in droplets vs. bulk) associated with the distinctive features of the interfacial environment.<sup>14,15</sup> Interfacial effects are readily observed in microdroplets because the large surface/volume ratios<sup>14–17</sup> which allow organic and sometimes inorganic reactions to be followed by spray based mass spectrometry (MS).<sup>18</sup> Several factors have been considered as contributing to reaction acceleration,<sup>14,15</sup> all associated with the special properties at the interface: they include partial solvation,<sup>14,15,17,19</sup> ordered molecular orientation,<sup>20–23</sup> confinement of reagent(s),<sup>24,25</sup> and

extremes of pH.<sup>26–28</sup> Most studies of reaction acceleration have been done in organic solvents but aqueous droplet reactions are also well represented.<sup>29–33</sup> Active species generated in the dielectric layer at the surface of water microdroplets include free radicals and hydrogen peroxide.<sup>29,30,34</sup> In very significant work, the strong electric field at the surface of aqueous droplets was recognized as playing a crucial role in reaction acceleration due to hydronium and hydroxide ion formation by ready auto-ionization of water at the surface.<sup>35</sup> In these circumstances, the hydronium ion appears to act as a superacid.<sup>32</sup> Significantly, even for organic solvents, trace amounts of water have been implicated in reaction acceleration, *e.g.* in benzimidazole formation from aromatic diamines and simple carboxylic acids.<sup>28</sup> The key step in this latter reaction is believed to be the protonation of simple acids like formic acid, followed by nucleophilic attack at carbon and then elimination of water.<sup>28</sup>

In the present study we probe carbon dioxide reactions with amines, expecting that protonation of CO<sub>2</sub> will be followed by C–N bond formation. Electrospray ionization was implemented to conduct microdroplet reactions and analyze the reaction products, as is now a common procedure.<sup>36–38</sup> However, in this study, the two reagents are introduced from different phases (liquid and gas) in order to study only reactions at the microdroplet interface. The CO<sub>2</sub> functionalization described involves gentle conditions that meets many of the requirements for ‘ideal CO<sub>2</sub> functionalization’ as set out in a recent study.<sup>39</sup>

## Results and discussion

### Amine reactions with CO<sub>2</sub> in room air

When a solution of *N,N*-dibutyl-1,3-propanediamine (DBPA) in acetonitrile was subjected to nanoelectrospray ionization

Department of Chemistry, Purdue University, West Lafayette, IN 47907, USA. E-mail: cooks@purdue.edu

† Electronic supplementary information (ESI) available. See DOI: 10.1039/d0sc05625a



(nESI), the protonated molecule (M) was observed as the ion  $[M + H]^+$  in the positive mode while the dominant species detected in the negative ion mode was the ion  $[M + 43]^-$  (see ESI, Fig. S1†), ascribed to  $[M - H + CO_2]^-$ . To determine whether this species is covalently bonded or simply a weakly bound ion/molecule complex of DBPA and carbon dioxide, we performed tandem mass spectrometry. The mass-selected precursor ion only fragmented at high collision energy and even then, the major product did not correspond to the loss of carbon dioxide. The observed fragments are formed by loss of alkane and alkene of the butyl group through charge-remote fragmentation,<sup>40</sup> followed by loss of imine. These facts, together with details of the fragmentation pattern, demonstrate that the species is the carbamate anion resulting from covalent bond formation between the amine nitrogen and carbon of CO<sub>2</sub> (note that although exact mass measurement were not available, tandem mass data provides a better identification of ion structure). A tentative proposal, justified below, is that carbamate formation occurs during the millisecond flight time of the droplets. After generation of the microdroplets, the hydrophobic amine at the surface of the charged droplets reacts with carbon dioxide from the atmosphere to form the carbamic acid which is subsequently detected by the MS.

### Effects of basicity and sterics

To scrutinize the mechanism and the factors that affect the reaction between amines and carbon dioxide in microdroplets, we sprayed amines of several types including primary amines, secondary amines, tertiary amines and diamines (listed in ESI, Scheme S1†). It is significant that CO<sub>2</sub> was not used as a reagent in these experiments: the only source of CO<sub>2</sub> was room air. The results are summarized in Table S1† and representative mass spectra are shown in Fig. S2.† The importance of the basicity of the reagent is indicated by the fact that the studied aliphatic amines gave  $[M - H + CO_2]^-$  ions but the aromatic amines, *N*-phenyldiamine, 1-naphthylamine, and 1,5-diaminonaphthalene, did not. These results also imply that the steric effect dominates the reaction by affecting the nucleophilicity of nitrogen (detailed discussion appears in the ESI†).

### Effect of deliberate addition of CO<sub>2</sub>

After studying the effect of choice of amine on the reaction with CO<sub>2</sub> in air, we examined the effect of adding carbon dioxide. We added carbon dioxide in three ways (i) by adding bicarbonate to the solution, (ii) by dropping dry ice into the solution and (iii) by bubbling carbon dioxide gas through the solution (Fig. S6†). Addition of bicarbonate had only a minor effect on the nESI mass spectra. After adding dry ice or bubbling CO<sub>2</sub>, we observed the carbamate (*m/z* 229) as well as an adduct  $[M + 43 + 44]^-$  (*m/z* 273 in Fig. S6f and h†) in the negative mode. Tandem mass spectrometry confirmed that this latter ion was a weak complex, as shown by the loss of mass 44 Da (CO<sub>2</sub>) at very low collision energy (Fig. S7†). A striking finding is the observation of a  $[M + 45]^+$  peak in the positive mode after intentionally adding carbon dioxide (Fig. S6e and g†); this species was not a weak adduct but was identified as protonated carbamic acid by tandem mass

spectrometry (Fig. S7†). The successive losses of CO<sub>2</sub> and NH<sub>3</sub> correspond to expected fragmentations of the carbamic acid functional group, while another diagnostic fragment corresponds to C–N cleavage at the tertiary nitrogen group. The experiment of adding an external source of carbon dioxide confirmed that gaseous carbon dioxide was involved in the formation of carbamic acid but it does not prove that the reaction occurs at the interface, a subject now taken up.

### Interfacial addition of CO<sub>2</sub> using ESSI

In an attempt to achieve a deeper understanding of the reaction, which we propose to occur at the droplet interface during flight, we implemented electrosonic spray ionization (ESSI) and utilized carbon dioxide as the nebulization gas (Fig. 1, S8 and S9†).<sup>41</sup> This methodology ensures that carbon dioxide makes contact with the amine only after generation of the microdroplets, ensuring that the reaction only occurs in the droplet environment. Importantly, the reaction is limited to near the gas–liquid interface rather than occurring throughout the whole droplet. From the estimated droplet diameter (3–6 μm for initial droplet and at least 2.7 μm after evaporation during flight)<sup>42</sup> and the estimated diffusion distance into the droplet (0.63 μm; see ESI p. S12†) only the near-surface region of the interface is accessible.

We explored carbon dioxide assisted ESSI using five representative amines of different types: octylamine (primary amine), dibutylamine (secondary amine), *N,N*-dibutyl-1,3-propanediamine (diamine with primary and tertiary amine), *N,N*-diethylethylenediamine (diamine with primary and tertiary amine), as well as *N,N'*-diethylethylenediamine (diamine with two secondary amines). Compared to a control experiment using N<sub>2</sub>, the use of CO<sub>2</sub> as nebulization gas results in C–N bond formation and its products are detected in both positive and negative ion modes (Fig. S8 and S9†). Protonated carbamic acid, at  $[M + 45]^+$ , was detected for the reactions of all the diamines (Fig. S8†). Correspondingly, carbamate anion was detected with dramatically increased signal/noise when supplying interfacial CO<sub>2</sub> compared to atmospheric CO<sub>2</sub> (Fig. S9†). Moreover, we observed a marked distance effect that further supports the hypothesis of reaction at the droplet surface (Fig. 2, S10 and S11†). Longer distances between the sprayer and the inlet of the mass spectrometer gave higher conversions of reagent to carbamic acid product and when varying the distance dynamically, by moving the sprayer backward and then forward (Fig. 2c and d) the conversion ratio and the relative intensity of protonated carbamic acid changed correspondingly. The absolute intensity of the reactant ion will decrease when increasing the distance, while the intensity of the product ions will increase somewhat resulting in a net large increase in conversion ratio intensity. Likewise, the detection of carbamate anion in the negative mode displayed similar distance results (Fig. 2b and S11†).

The above mentioned results provide strong evidence that C–N bond formation between amines and carbon dioxide happens during the flight of the droplet, meaning that the reaction occurs on the microsecond to millisecond timescale. One incidental observation is that during the flight of the





Fig. 1 DBPA/CO<sub>2</sub> droplet reaction by adding CO<sub>2</sub> in the gas phase (a) Droplet reaction of amine/CO<sub>2</sub> conducted by ESSI. (b) Positive and (c) negative mode mass spectra and MS/MS spectra showing fragmentation of protonated and deprotonated DBPA carbamic acid.

droplet containing DBPA, three water molecules (due to ambient humidity) are captured to form an ion  $m/z$  241. A suggested structure of this magic number hydrate is given in the ESI (Fig. S12<sup>†</sup>).

Encouraged by the above findings, we used DBPA as a model amine to conduct a concentration-dependent experiment (Fig. S13<sup>†</sup>). Unlike the results for nanoESI (Fig. S4b<sup>†</sup>) or N<sub>2</sub> assisted ESSI (Fig. S13a<sup>†</sup>) at low amine concentration, carbamate anion was the dominant product in droplet reactions using CO<sub>2</sub> assisted ESSI even at low amine concentrations (Fig. 1 and S13e<sup>†</sup>). Moreover, by conducting droplet reactions using interfacial CO<sub>2</sub>, the signal to noise ratio was greatly enhanced (Fig. S13f and h<sup>†</sup>) compared to N<sub>2</sub> assisted ESSI (even when the latter experiment was performed using higher amine concentrations, Fig. S13b and d<sup>†</sup>). A superficially surprisingly

result is that the conversion ratio of DBPA increased as its concentration was decreased (Fig. S14, S15 and Table S2<sup>†</sup>). Kinetically, higher concentrations of amine give rise to higher reaction rates. However, our results suggest that the acceleration factor for lower concentrations is higher in the microdroplets. This counterintuitive result is highly characteristic of accelerated droplet reactions including the Katritzky transamination reaction in Leidenfrost and microdroplets.<sup>17,34</sup> These previous studies, performed using surface active reagents, showed that lower concentrations lead to higher acceleration factors at low concentrations because the overall rate is dominated by reactions at the air/solution interface (reaction acceleration is an interfacial phenomenon associated strongly with partial solvation, as evidenced by experiment<sup>14,15,17,19</sup> and supported by high level calculations.<sup>23</sup>) This explanation suggests



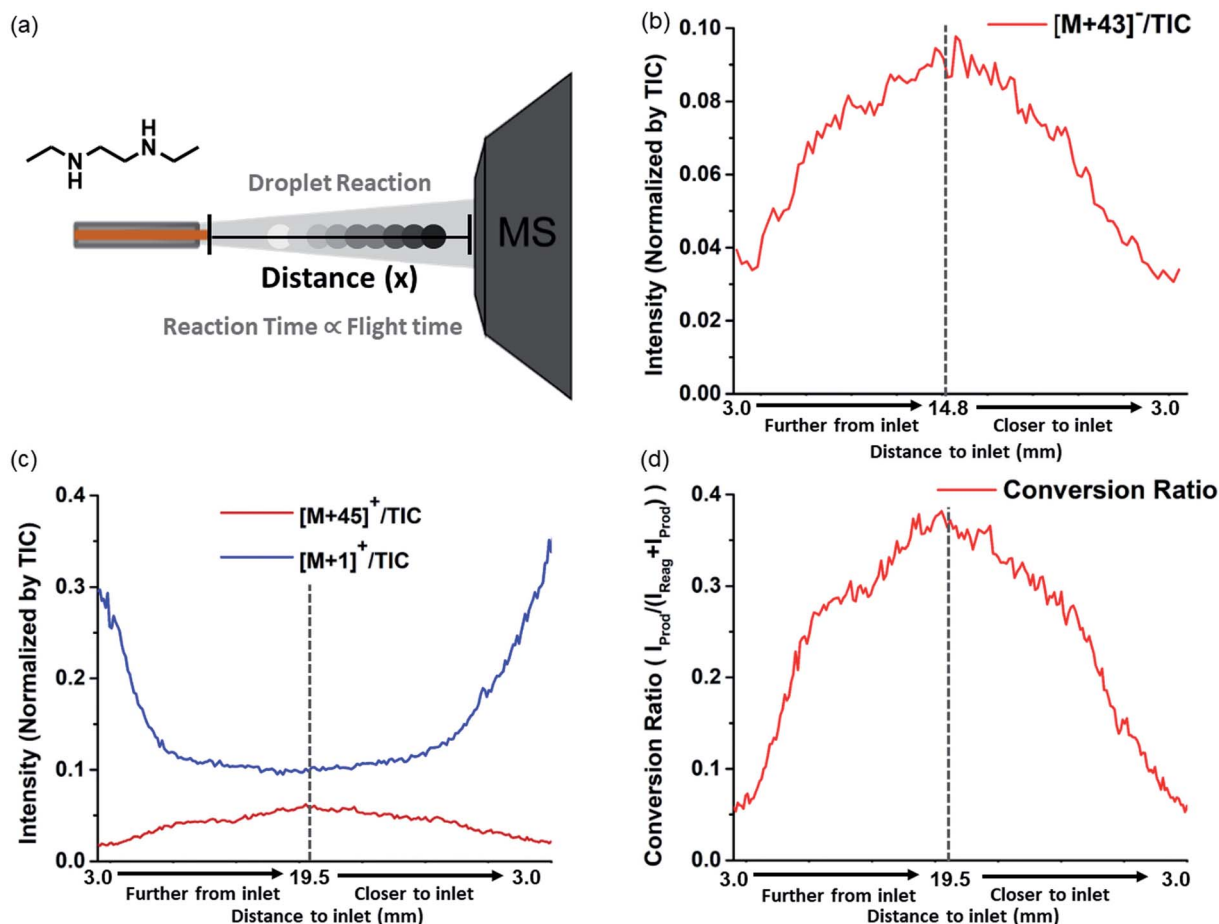


Fig. 2 Distance effect of *N,N'*-diethylenediamine. (a) Experimental setup of the distance-dependent effect. Moving forward decreases the distance between the sprayer and the inlet while moving backward increases this distance. Plots as function of distance between sprayer and MS inlet show (b) absolute intensity of carbamate anion  $[M + 43]^-$ , (c) normalized signal of protonated DBPA  $[M + 45]^+$  and signal of protonated carbamic acid  $[M + 41]^+$ , (d) conversion ratio of DBPA to carbamate in positive mode.

that most of the carbon dioxide reacts with the amine at the interface rather than diffusing into the droplet for reaction, emphasizing the role of interfacial microdroplet reactions.

To gain further insight into the role of interfacial chemistry, we probed the difference between providing  $\text{CO}_2$  from the liquid–gas interface and from the solution. When carbon dioxide is injected into the solution and then the solution is nebulized using  $\text{N}_2$ , the  $\text{CO}_2$  source in the solution must reach the interface for accelerated reaction to occur (Fig. S16 and S17<sup>†</sup>), while spraying analyte with the assistance of  $\text{CO}_2$  nebulizing gas provides  $\text{CO}_2$  directly to the liquid–gas interface (Fig. 1a). Considering the formation of carbamic acid and detection in the positive mode,  $\text{CO}_2$  provided only at the interface will be affected significantly by the interfacial effect, causing the concentration effect (already noted above) of giving higher conversion ratios at lower concentration (Fig. S15<sup>†</sup>). However, the uniform distribution of  $\text{CO}_2$  in the solution in the case of injected  $\text{CO}_2$  means that the slower bulk reaction (interior) should dominate (Fig. S16<sup>†</sup>). These expectations indeed match the observations. The detection of product in the negative mode also revealed strong differences between

providing  $\text{CO}_2$  at the interface or in solution. A species corresponding to the ion/molecule cluster of  $\text{CO}_2$  and carbamate ( $m/z$  273 in Fig. S17<sup>†</sup>) was detected in the case of providing  $\text{CO}_2$  from solution. This is rationalized by the fact that excess  $\text{CO}_2$  can form ion/molecule clusters after forming carbamate. However, if the carbamate were formed at the interface of ESSi and then diffused into the droplet, the carbamate– $\text{CO}_2$  cluster would not be expected and is not detected in the case of interfacial  $\text{CO}_2$  (Fig. 1 and S13<sup>†</sup>). These comparisons reinforce the role of the interface in carbamic acid formation and its detection in both the positive and the negative mode.

#### Mechanistic considerations: are there contributions from gas phase ion/molecule reactions?

There has been some discussion of whether ion/molecule reactions in the gas phase might contribute to or be responsible for accelerated reactions in microdroplets.<sup>43</sup> While the effect of evaporation is recognized, the increase in rate constant associated with accelerated reactions in microdroplets provides independent data on this point. The case for a gas phase ion/molecule reaction contribution to amine carboxylation as



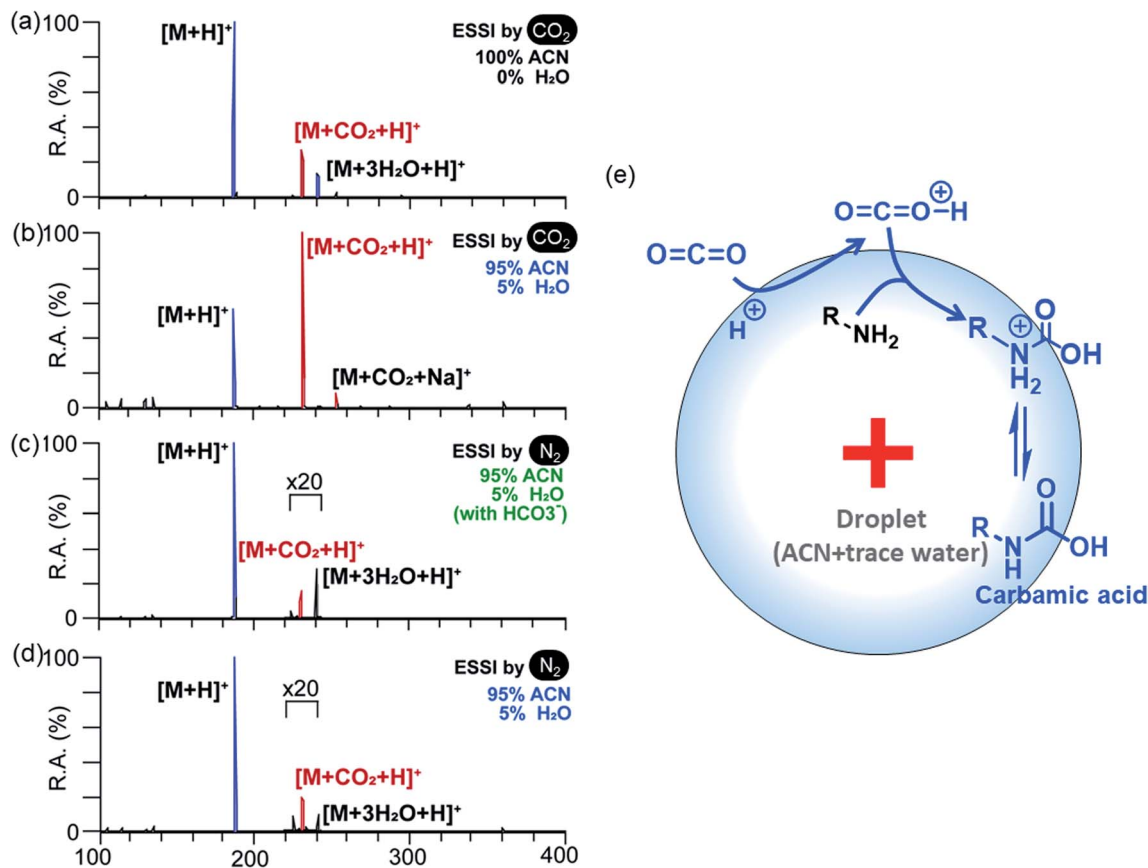


Fig. 3 Droplet reaction showing positive ion ESSI mass spectra of (a) ACN droplets and (b) 5% water in ACN droplets with interfacial  $\text{CO}_2$  (c) 5% water in ACN droplets bicarbonate (added) and (d) droplet reaction of 5% water in ACN droplets with room  $\text{CO}_2$ . (e) Mechanistic description of room air  $\text{CO}_2$ /amine droplet reaction (ACN with small amounts of water). Autoionization at the charged interface gives superacid which protonates  $\text{CO}_2$ , allowing reaction with amine to form the carbamic acid, the protonated form of which is observed at  $m/z$  231 in the mass spectrum.

observed in this study has been further examined by assembling arguments and additional experimental data which is shown in the ESI† (Section 7). During the flight of the droplets, several events might contribute to gas phase ion/molecule reactions.

(1) Complete evaporation of solvent to produce charged amines.

(2) Evaporation of volatile reagents into the gas phase where they react with  $\text{CO}_2$ .

(3) Droplet fission and evaporation of solvent (or direct ion evaporation) to generate gas phase ions that then undergo ion/molecule reactions with  $\text{CO}_2$ .

(4) Desolvation of droplets in the MS inlet and subsequent ion/molecule reactions in the inlet.

The evaporation of acetonitrile droplets of 3  $\mu\text{m}$  diameter during the 2 cm flight distance can reduce their diameters but only to 2.7  $\mu\text{m}$  (see ESI, Section 7†). Evaporation of the volatile amines might occur but a non-volatile amine for which a gas phase reaction is not possible showed a very similar reactivity (Fig. S21†). Addressing the third point, coulombic fission can lead to small offspring droplets that might evaporate rapidly and be involved in gas phase ion/molecule reactions. To assess the degree to which this might occur we compared data for gas

phase amines with that for amines in droplets, using the same apparatus (Fig. S22†). The results show a very small gas phase reaction when compared to the droplet reaction. Finally, the MS inlet temperature was changed over a wide range (Fig. S23†) and this had little effect on the intensity of the carbamate product, indicating that little reaction is occurring in the vapor phase. We conclude that amine carboxylation occurs to an overwhelming extent at the surface of the microdroplets.

#### Further mechanistic considerations

To rationalize the distinctive chemistry in the microdroplet when providing  $\text{CO}_2$  at the interface, we consider several possible mechanisms (Scheme S2†) for carbamic acid formation: (1) nucleophilic attack of amine on  $\text{CO}_2$  to form the zwitterion; (2)  $\text{CO}_2$  protonation by superacid generated at the droplet surface, followed by amine attack at the activated carbonium ion and (3) reaction of the free amine with  $\text{CO}_2$  at the interface; (4) amine deprotonation by a superbases at the interface followed by subsequent nucleophilic attack on carbon dioxide. Reactions (1) and (3) are energetically unlikely. The protonated carbon dioxide and deprotonated amine reactions are of special interest because these forms of the reagents could





Fig. 4 Droplet reaction showing negative ion ESSI mass spectra of (a) ACN droplets and (b) 5% water in ACN droplets with interfacial  $CO_2$  (c) 5% water in ACN droplets bicarbonate (added) and (d) droplet reaction of 5% water in ACN droplets with room  $CO_2$ . Autoionization at the charged interface gives superbase which deprotonates the amine, allowing reaction with  $CO_2$  to form the carbamate anion. (e) Mechanism of superacid/superbase assisted carbamic acid formation at the droplet interface. Small amounts of water present in the droplet generate superacid/superbase at the interface in the presence of a high field, and subsequently activate the carbon dioxide/amine by protonating the carbon dioxide/deprotonating the amine. Note that the species proposed here are the ionic species at the reacting functional groups.

arise from superacid/superbase reactions at the interface as discussed in the Introduction.<sup>28</sup>

Previous reports<sup>28,30-34</sup> have suggested that superacid (extreme pH) at the interface of organic droplets (and dielectric layers at the interface of water microdroplets) accelerate reactions. These results indicated the importance of water, even traces of water<sup>28</sup> in interfacial microdroplet chemistry. In the light of these results, we propose that  $CO_2$  at the surface will be protonated due to interfacial water acting as a superacid and so forming carbamic acid. To test this hypothesis, we conducted experiments with different amounts of water in acetonitrile. Fig. S18, S19, and Table S3† summarize the conversion ratio of DBPA to the carbamic acid using water in acetonitrile, especially small amounts of water. Trace amounts of water (5%) in the organic solvent enhanced the production of carbamic acid dramatically from 20% to 60% on the millisecond time scale, while the reaction is impeded with larger proportions of water (conversion ratio is *ca.* 10% when 50% water is added) (see ESI Section 6 and Table S4† for a detailed discussion of acceleration factors under different circumstances, including bulk reaction,

microdroplet reaction, and superacid/superbase driven microdroplet reactions).

Considering this result, and previous reports, we propose an acceleration mechanism involving (i) partial solvation of reagents at the surface and (ii) autoionization of water at the gas/liquid interface to provide superacid/superbase reagents. The partial solvation of reagents lowers the activation energy increasing the rate constant at the surface relative to the bulk reaction. Moreover, the trace amount of water at the interface of the microdroplet generates a hydronium/hydroxide dielectric layer, which then act as the superacid/superbase because of partial solvation. These surface-active species (superacid/superbase) further enhance the reaction rate (Fig. 3 and 4). Comparing Fig. 3a and b, the conversion ratio is greatly enhanced in the presence of trace water. Similarly, in Fig. 4a and b, trace water was observed to increase the carbamate anion signal.

The proposed mechanisms based on trace amounts water are summarized in Fig. 3e and 4e. Briefly, superacid at the surface (surface protons) protonate carbon dioxide, increasing



the electrophilicity of carbon and facilitating nucleophilic addition. Meanwhile, superacid at the surface implies the existence of superbase at the surface, and we propose that the superbase deprotonates the amine, making it much more reactive than the neutral amine (Fig. 4a and b). However, a large amount of water prevents the nucleophilic addition and lowers the conversion ratio. Although the reaction of CO<sub>2</sub> with amine was extremely fast at the interface of microdroplets under trace amounts of water, there is still a possibility that the reaction is driven by dissolved CO<sub>2</sub> in the form of carbonic acid/bicarbonate. To test this, we added sodium carbonate to the solution and conducted the microdroplet reaction using N<sub>2</sub> as nebulization gas (Fig. 3c, cf. Fig. 3a and b). Note that we added bicarbonate instead of carbonic acid because lowering the pH will impede the reaction and CO<sub>2</sub> dissolved in basic condition will form bicarbonate. As shown in Fig. S3c,† carbamic acid was barely observable in this case (the small amount of carbamic acid formed is no different to that seen when simply spraying the same solution without bicarbonate, Fig. 3d). Fig. 3c and d show that the amine microdroplet itself can capture room CO<sub>2</sub> and that bicarbonate representing the dissolved CO<sub>2</sub> in solution will not increase the formation of carbamic acid. These results indicate that the majority of the reaction in CO<sub>2</sub> assisted ESSI with trace amounts of water was not from the bicarbonate generated by CO<sub>2</sub> dissolved in surface region water under basic conditions. Fig. 3e summarizes the mechanistic effects of trace amounts of water, suggesting that the distinctive enhancement of product formation is mainly due to protonation of CO<sub>2</sub> at the surface rather than dissolved form of CO<sub>2</sub>. Similarly, the presence of trace water assists in the formation of the carbamate anion (Fig. 4c and d). All the above results strengthen the conclusion that the distinct interfacial chemistry in microdroplets containing trace amounts of water is driven by the formation of superacid/superbase at the interface.

## Conclusion

We investigated carbamic acid formation by amine/CO<sub>2</sub> reaction in droplets and specifically the interfacial chemistry. The reaction of CO<sub>2</sub> with amine was investigated for the intrinsic properties of the amine, the concentration of amine, the source of carbon dioxide, and the effect of pH on reaction with room air CO<sub>2</sub>. By using carbon dioxide as nebulization gas, we provided evidence for the hypothesis that the reaction occurred near the surface of the droplet during its flight. Distance of flight experiments supported this argument. Most intriguingly, reaction near the interface was probed by adding different amounts of water, and the results indicated that a trace amount of water in an organic solvent can dramatically enhance carbamic acid production. We propose that the enhancement is due to the superacid/superbase properties of an aqueous surface that can activate the functional groups involved in the reaction. This work indicates that droplet reactions can be used to facilitate the screening of reagents for carbon dioxide capture and storage. The role of superacid chemistry when using organic solvents with small amounts of water has been extended from imidazole formation<sup>28</sup> to carbamic acid formation in this work.

The suggestion that superbase drives this reaction deserves to be tested by seeking other reactions in which strong nucleophiles (RHN<sup>-</sup>, RS<sup>-</sup> etc.) might serve as reagents.

## Conflicts of interest

There are no conflicts to declare.

## Acknowledgements

This work was supported by the National Science Foundation 19-05087. The authors thank Prof. Yan Xin (Texas A&M University) for providing key suggestions.

## References

- I. A. Berg, Ecological aspects of the distribution of different autotrophic CO<sub>2</sub> fixation pathways, *Appl. Environ. Microbiol.*, 2011, **77**(6), 1925–1936.
- G. P. Peters, G. Marland, C. Le Quéré, T. Boden, J. G. Canadell and M. R. Raupach, Rapid growth in CO<sub>2</sub> emissions after the 2008–2009 global financial crisis, *Nat. Clim. Change*, 2012, **2**(1), 2–4.
- S. Dabral and T. Schaub, The use of carbon dioxide (CO<sub>2</sub>) as a building block in organic synthesis from an industrial perspective, *Adv. Synth. Catal.*, 2019, **361**(2), 223–246.
- J. Artz, T. E. Muller, K. Thenert, J. Kleinekorte, R. Meys, A. Sternberg, A. Bardow and W. Leitner, Sustainable Conversion of Carbon Dioxide: An Integrated Review of Catalysis and Life Cycle Assessment, *Chem. Rev.*, 2018, **118**(2), 434–504.
- A. Tortajada, F. Julia-Hernandez, M. Borjesson, T. Moragas and R. Martin, Transition-Metal-Catalyzed Carboxylation Reactions with Carbon Dioxide, *Angew. Chem., Int. Ed. Engl.*, 2018, **57**(49), 15948–15982.
- D. M. D'Alessandro, B. Smit and J. R. Long, Carbon dioxide capture: prospects for new materials, *Angew. Chem., Int. Ed. Engl.*, 2010, **49**(35), 6058–6082.
- D. Y. Leung, G. Caramanna and M. M. Maroto-Valer, An overview of current status of carbon dioxide capture and storage technologies, *Renew. Sustain. Energy Rev.*, 2014, **39**, 426–443.
- X. Shi, H. Xiao, H. Azarabadi, J. Song, X. Wu, X. Chen and K. S. Lackner, Sorbents for the Direct Capture of CO<sub>2</sub> from Ambient Air, *Angew. Chem., Int. Ed. Engl.*, 2020, **59**(18), 6984–7006.
- G. Puxty, R. Rowland, A. Allport, Q. Yang, M. Bown, R. Burns, M. Maeder and M. Attalla, Carbon dioxide postcombustion capture: a novel screening study of the carbon dioxide absorption performance of 76 amines, *Environ. Sci. Technol.*, 2009, **43**(16), 6427–6433.
- I. Niedermaier, M. Bahlmann, C. Papp, C. Kolbeck, W. Wei, S. Krick Calderon, M. Grabau, P. S. Schulz, P. Wasserscheid, H. P. Steinruck and F. Maier, Carbon dioxide capture by an amine functionalized ionic liquid: fundamental differences of surface and bulk behavior, *J. Am. Chem. Soc.*, 2014, **136**(1), 436–441.



- 11 T. M. McDonald, J. A. Mason, X. Kong, E. D. Bloch, D. Gygi, A. Dani, V. Crocella, F. Giordanino, S. O. Odoh, W. S. Drisdell, B. Vlasisavljevich, A. L. Dzubak, R. Poloni, S. K. Schnell, N. Planas, K. Lee, T. Pascal, L. F. Wan, D. Prendergast, J. B. Neaton, B. Smit, J. B. Kortright, L. Gagliardi, S. Bordiga, J. A. Reimer and J. R. Long, Cooperative insertion of CO<sub>2</sub> in diamine-appended metal-organic frameworks, *Nature*, 2015, **519**(7543), 303–308.
- 12 V. Y. Mao, P. J. Milner, J. H. Lee, A. C. Forse, E. J. Kim, R. L. Siegelman, C. M. McGuirk, L. B. Porter-Zasada, J. B. Neaton, J. A. Reimer and J. R. Long, Cooperative Carbon Dioxide Adsorption in Alcoholamine- and Alkoxyalkylamine-Functionalized Metal-Organic Frameworks, *Angew. Chem., Int. Ed. Engl.*, 2019, **59**(44), 19468–19477.
- 13 M. Aresta, A. Dibenedetto and A. Angelini, Catalysis for the valorization of exhaust carbon: from CO<sub>2</sub> to chemicals, materials, and fuels. technological use of CO<sub>2</sub>, *Chem. Rev.*, 2014, **114**(3), 1709–1742.
- 14 X. Yan, R. M. Bain and R. G. Cooks, Organic reactions in microdroplets: Reaction acceleration revealed by mass spectrometry, *Angew. Chem., Int. Ed.*, 2016, **55**(42), 12960–12972.
- 15 Z. Wei, Y. Li, R. G. Cooks and X. Yan, Accelerated Reaction Kinetics in Microdroplets: Overview and Recent Developments, *Annu. Rev. Phys. Chem.*, 2020, **71**, 31–51.
- 16 Y. Li, X. Yan and R. G. Cooks, The Role of the Interface in Thin Film and Droplet Accelerated Reactions Studied by Competitive Substituent Effects, *Angew. Chem., Int. Ed. Engl.*, 2016, **55**(10), 3433–3437.
- 17 Y. Li, T. F. Mehari, Z. Wei, Y. Liu and R. G. Cooks, Reaction acceleration at air-solution interfaces: Anisotropic rate constants for Katritzky transamination, *J. Mass Spectrom.*, 2020, e4585.
- 18 J. Cao, Q. Wang, S. An, S. Lu and Q. Jia, Facile and efficient preparation of organoimido derivatives of [Mo6O19]<sup>2-</sup> using accelerated reactions in Leidenfrost droplets, *Analyst*, 2020, **145**(14), 4844–4851.
- 19 S. Vaitheeswaran and D. Thirumalai, Hydrophobic and ionic interactions in nanosized water droplets, *J. Am. Chem. Soc.*, 2006, **128**(41), 13490–13496.
- 20 I. Nam, J. K. Lee, H. G. Nam and R. N. Zare, Abiotic production of sugar phosphates and uridine ribonucleoside in aqueous microdroplets, *Proc. Natl. Acad. Sci. U. S. A.*, 2017, **114**(47), 12396–12400.
- 21 I. Nam, H. G. Nam and R. N. Zare, Abiotic synthesis of purine and pyrimidine ribonucleosides in aqueous microdroplets, *Proc. Natl. Acad. Sci. U. S. A.*, 2018, **115**(1), 36–40.
- 22 Z. Zhou, X. Yan, Y. H. Lai and R. N. Zare, Fluorescence Polarization Anisotropy in Microdroplets, *J. Phys. Chem. Lett.*, 2018, **9**(11), 2928–2932.
- 23 N. Narendra, X. Chen, J. Wang, J. Charles, R. G. Cooks and T. Kubis, Quantum Mechanical Modeling of Reaction Rate Acceleration in Microdroplets, *J. Phys. Chem. A*, 2020, **124**(24), 4984–4989.
- 24 A. Fallah-Araghi, K. Meguellati, J.-C. Baret, A. El Harrak, T. Mangeat, M. Karplus, S. Ladame, C. M. Marques and A. D. Griffiths, Enhanced chemical synthesis at soft interfaces: A universal reaction-adsorption mechanism in microcompartments, *Phys. Rev. Lett.*, 2014, **112**(2), 028301.
- 25 N. Sahota, D. I. AbuSalim, M. L. Wang, C. J. Brown, Z. Zhang, T. J. El-Baba, S. P. Cook and D. E. Clemmer, A microdroplet-accelerated Biginelli reaction: mechanisms and separation of isomers using IMS-MS, *Chem. Sci.*, 2019, **10**(18), 4822–4827.
- 26 M. Girod, E. Moyano, D. I. Campbell and R. G. Cooks, Accelerated bimolecular reactions in microdroplets studied by desorption electrospray ionization mass spectrometry, *Chem. Sci.*, 2011, **2**(3), 501–510.
- 27 S. Banerjee and R. N. Zare, Syntheses of Isoquinoline and Substituted Quinolines in Charged Microdroplets, *Angew. Chem., Int. Ed. Engl.*, 2015, **54**(49), 14795–14799.
- 28 P. Basuri, L. E. Gonzalez, N. M. Morato, T. Pradeep and R. G. Cooks, Accelerated microdroplet synthesis of benzimidazoles by nucleophilic addition to protonated carboxylic acids, *Chem. Sci.*, 2020, **10**(47), 12686–12694.
- 29 J. K. Lee, D. Samanta, H. G. Nam and R. N. Zare, Spontaneous formation of gold nanostructures in aqueous microdroplets, *Nat. Commun.*, 2018, **9**(1), 1562.
- 30 D. Gao, F. Jin, J. K. Lee and R. N. Zare, Aqueous microdroplets containing only ketones or aldehydes undergo Dakin and Baeyer-Villiger reactions, *Chem. Sci.*, 2019, **10**(48), 10974–10978.
- 31 E. Gnanamani, X. Yan and R. N. Zare, Chemoselective N-Alkylation of Indoles in Aqueous Microdroplets, *Angew. Chem., Int. Ed. Engl.*, 2020, **59**(8), 3069–3072.
- 32 K. Luo, J. Li, Y. Cao, C. Liu, J. Ge, H. Chen and R. N. Zare, Reaction of chloroauric acid with histidine in microdroplets yields a catalytic Au-(His)<sub>2</sub> complex, *Chem. Sci.*, 2020, **11**(9), 2558–2565.
- 33 X. Zhong, H. Chen and R. N. Zare, Ultrafast enzymatic digestion of proteins by microdroplet mass spectrometry, *Nat. Commun.*, 2020, **11**(1), 1049.
- 34 J. K. Lee, D. Samanta, H. G. Nam and R. N. Zare, Micrometer-Sized Water Droplets Induce Spontaneous Reduction, *J. Am. Chem. Soc.*, 2019, **141**(27), 10585–10589.
- 35 H. Xiong, J. K. Lee, R. N. Zare and W. Min, Strong Electric Field Observed at the Interface of Aqueous Microdroplets, *J. Phys. Chem. Lett.*, 2020, **11**(17), 7423–7428.
- 36 R. D. Espy, M. Wlekinski, X. Yan and R. G. Cooks, Beyond the flask: reactions on the fly in ambient mass spectrometry, *TrAC, Trends Anal. Chem.*, 2014, **57**, 135–146.
- 37 A. J. Ingram, C. L. Boeser and R. N. Zare, Going beyond electrospray: mass spectrometric studies of chemical reactions in and on liquids, *Chem. Sci.*, 2016, **7**(1), 39–55.
- 38 R. G. Cooks and X. Yan, Mass spectrometry for synthesis and analysis, *TrAC, Trends Anal. Chem.*, 2018, **11**, 1–28.
- 39 Y. Yang and J.-W. Lee, Toward ideal carbon dioxide functionalization, *Chem. Sci.*, 2019, **10**(14), 3905–3926.
- 40 M. L. Gross, Charge-remote fragmentations: method, mechanism and applications, *Int. J. Mass Spectrom. Ion Processes*, 1992, **118**, 137–165.
- 41 Z. Takats, J. M. Wiseman, B. Gologan and R. G. Cooks, Electrosonic spray ionization. A gentle technique for





- generating folded proteins and protein complexes in the gas phase and for studying ion-molecule reactions at atmospheric pressure, *Anal. Chem.*, 2004, **76**(14), 4050–4058.
- 42 A. Venter, P. E. Sojka and R. G. Cooks, Droplet dynamics and ionization mechanisms in desorption electrospray ionization mass spectrometry, *Anal. Chem.*, 2006, **78**(24), 8549–8555.
- 43 G. Rovelli, M. I. Jacobs, M. D. Willis, R. J. Rapf, A. M. Prophet and K. R. Wilson, A critical analysis of electrospray techniques for the determination of accelerated rates and mechanisms of chemical reactions in droplets, *Chem. Sci.*, 2020, DOI: 10.1039/d0sc04611f.

